

Analytical Models of Axisymmetric Toroidal Magnetic Fields with Noncircular Flux Surfaces

V.A.Yavorskij^a, K.Schoepf^b, Zh.N.Andrushchenko^a, B.H.Cho^b,
V.Ya.Goloborod'ko^a, S.N.Reznyk^a

^a*Institute for Nuclear Research, Ukrainian Academy of Sciences, Kiev, Ukraine*

^b*Institute for Theoretical Physics, University of Innsbruck, Austria*

1. INTRODUCTION

The present paper provides an analytical model of tokamak fields with noncircular (triangular) and up-down asymmetric magnetic surfaces of arbitrary aspect ratio and its adaptation to real equilibrium fields. Our objective here is to accurately describe the tokamak magnetic configuration with a minimum number of parameters determining the shape and position of flux surfaces (FSs).

2. TOKAMAK MAGNETIC FIELD WITH PRESCRIBED FLUX SURFACES

In what follows, we refer to a prescribed axisymmetric magnetic field $\mathbf{B}(R,Z)$ with the flux surfaces determined by the parametric dependence of the cylindrical coordinates

$$R = R(\chi, r, \Pi(r)); \quad Z = Z(\chi, r, \Pi(r)) \quad (1)$$

where R and Z represent the spatial variables of the cylindrical coordinate system $[R, Z, \varphi]$, r is the flux surface radius in the equatorial plane which contains the magnetic axis, χ is the poloidal angle, and $\Pi(r)$ denotes the set of parameters describing the flux surface position and shape. As evident from Fig. 1, $R = R_0(r)$ marks the FS centre in the equatorial plane and, hence, the magnetic axis is specified by $R = R_{ax} = R_0(0)$ and $Z = Z_{ax}$ designating the horizontal and the vertical position of the magnetic axis, respectively.

It can be shown that the magnetic field and the flux coordinates $[\Phi, \vartheta]$ are related to r and χ by

$$\mathbf{B}_t \equiv J\nabla\varphi = \nabla\Phi \times \nabla\vartheta = \hat{\vartheta}(r, \chi)\nabla\Phi \times \nabla\chi, \quad \mathbf{B}_p = q^{-1}(r)\nabla\varphi \times \nabla\Phi, \quad (2)$$

$$d\vartheta/d\chi \equiv \hat{\vartheta}(r, \chi) = Y(r, \chi)/\langle Y \rangle, \quad d\Phi/dr = J\langle Y \rangle, \quad Y(r, \chi) := \{R, Z\}/R, \quad \langle \dots \rangle \equiv \frac{1}{2\pi} \int d\chi(\dots); \quad (3)$$

here $[\Phi, \vartheta, \varphi]$ is the flux coordinate system with prescribed toroidal angle and straight field lines (so-called basic coordinate system for tokamaks [1]), $\Phi(r)$ is the toroidal magnetic flux (divided by 2π), $q(r)$ is the safety factor, $J(r)$ is the total poloidal current (divided by 2π) outside a given flux surface. We assume here – based on several geometric examinations of FSs – that the surface is predominantly shaped by the positions of the maximum and minimum points in the Z co-ordinate, $N(R_N, Z_N)$ and $S(R_S, Z_S)$ as displayed in Fig. 1, as well as by the positions of the two extreme points in the R -coordinate in the equatorial plane ($Z = Z_{ax}$). The latter points are indicated in Fig. 1 as $E(R_E, Z_{ax})$ and $W(R_W, Z_{ax})$. Thus we have six independent values $\{R_N, Z_N, R_S, Z_S, R_E, R_W\}$ to specify a given FS and, therefore, we may introduce six independent parameters for modelling the flux surface geometry. These are chosen to be the flux surface radius $r = (R_E(r) - R_W(r))/2$, the Shafranov shift $\Delta_e(r) = (R_E(r) + R_W(r) - R_E(a) - R_W(a))/2$ with a denoting the flux surface radius at the

separatrix, the elongation parameter $k_e(r) = (Z_N(r) - Z_S(r))/2r$, the triangularity parameter $\Lambda_e(r) = (R_E(r) + R_W(r) - R_N(r) - R_S(r))/2r$, and finally the parameter of vertical up-down asymmetry, $\eta_e(r) = (Z_N(r) + Z_S(r) - 2Z_{ax})/(Z_N(r) - Z_S(r))$, and that of horizontal up-down asymmetry, $\zeta_e(r) = (R_N(r) - R_S(r))/2r$. Hence, in addition to the flux surface radius r , we have five parameters to describe flux surface shapes, namely the set $\Pi_e(r) \equiv [\Delta_e(r), k_e(r), \Lambda_e(r), \eta_e(r), \zeta_e(r)]$ where the subscript "e" is used to indicate the effective measured value of a parameter. The profiles of Π_e typical for equilibrium flux surfaces in JET, NSTX and TCV [2] are displayed in Figs. 2-4. In general, elongated and triangular flux surfaces that are symmetric with respect to the equatorial plane (superscript S) may be represented by [2]

$$R = R^S(\chi, r, \Pi^S(r)) \equiv R^0(\chi, r, \Pi^0(r)) + \Delta R(\chi, r, \Pi^S(r)); \Pi^0(r) = \{\Delta(r), k(r)\} \quad (4)$$

$$Z = Z^S(\chi, r, \Pi^S(r)) \equiv Z^0(\chi, r, \Pi^0(r))T(\chi, r, \Pi^S(r)); \Pi^S(r) = \{\Pi^0(r), \Lambda(r)\} \quad (5)$$

where $R^0 \equiv R_c + \Delta(r) + r \cos \chi$ and $Z^0 \equiv k(r)r \sin \chi$, and the functions $\Delta R(\chi, r, \Pi^S(r))$ and $T(\chi, r, \Pi^S(r))$ are symmetric in Z - Z_{ax} and describe the deviations from the elliptic (circular) shape. In Table 1 we give three different analytical representations for $R = R^S(\chi, r, \Pi^S(r))$ and $Z = Z^S(\chi, r, \Pi^S(r))$ modelling three distinct classes of elongated and triangular flux surfaces.

Table 1. Analytical models of up-down symmetric triangular flux surfaces

Model	$\Delta R = R - R^0$	$T = Z / Z^0$	k/k_e	Λ/Λ_e
I	0	$[1 - \Lambda(r) \cos \chi]^\alpha$	$M [1 + (1 - M^2)/\alpha]^\alpha$	$M^2 / (\alpha + 1 - M^2)$
II	0	$\exp[-\Lambda(r) \cos \chi]$	$M \exp(1 - M^2)$	$M^2 = 1 / (1 - \Lambda_e^2)$
III	$-r\Lambda(r)\sin^2 \chi$	1	1	1

To take into account the vertical up-down asymmetry of flux surfaces we replace the expression for Z by $Z = Z^S K$ taking $K = (1 + \eta \sin \chi)$, where it is obvious that the term proportional to η introduces the vertical asymmetry of the FS elongation. Additionally, by means of interference of the factors T and K also the horizontal positions of the points N and S are varied, which introduces a horizontal asymmetry $\Delta\zeta$ in models I and II.

3. COMPARISON OF MODELLED WITH EQUILIBRIUM FLUX SURFACES

In this section our different flux surface models are evaluated by comparison with the equilibrium magnetic configurations in NSTX, JET and TCV. The mentioned variety of equilibrium FS shapes provides a good basis for testing the analytical models since, among

these tokamaks, the measured noncircularity parameters occurring in Π_e will alter also over a wide range.

Figures 5 and 6 display the modelled and the equilibrium flux surfaces for discharges in the low aspect ratio NSTX plasma with $\beta = 23\%$ and $\beta = 40\%$ featuring a weak horizontal asymmetry ($\zeta < 0.01$). It can be seen that flux surfaces associated with $\beta = 23\%$ are well described by model II, while in the case $\beta = 40\%$ the better agreement with the equilibrium surfaces is found for model I ($\alpha = -0.5$) and model III. In both discharges, the discrepancy between the analytically and numerically modelled flux surfaces is less than 5%, even for the outmost flux surfaces.

A comparison of model-III flux surfaces related to JET geometry with the actual equilibrium FSs of JET discharge #45341 ($t \sim 45$ s) is rendered by Fig. 7. This equilibrium plot differs essentially from NSTX configurations by a considerable asymmetry in the R direction because of the single X-point (saddle point of the separatrix) below the midplane. Although the applied analytical model does not consider horizontal asymmetry, the modelled FSs are found in excellent agreement with the measured ones over the entire cross section except in the vicinity of the X-point. There the maximum discrepancy between the model III-approximated and the actual equilibrium flux surface with $\Psi = 0.95\Psi_{\text{outermost}}$ is less than 10%. Finally Figs. 8 and 9 show the modelled and the equilibrium surfaces for TCV shots #16099 and #14388. Notwithstanding the drastic dissimilarity of the triangularity parameters of these shots ($\Lambda_{\text{edge}} = 0.22$ and, respectively, $\Lambda_{\text{edge}} = -0.43$) both equilibria could be satisfactorily approximated by the FS plots of model III.

4. CONCLUSION

The presented parametric modelling demonstrates the possibility of analytical description of axisymmetric toroidal magnetic fields with noncircular and up-down asymmetric flux surfaces of arbitrary aspect ratio by a minimum of four geometric parameters determining the shape and position of flux surfaces. Namely, these parameters are the Shafranov shift, the elongation, the triangularity and the up-down asymmetry. Additionally, a numerical shape constant distinguishing different models was used.

Acknowledgement

This study was performed partially within the Association EURATOM-OEAW Project P4 and under financial support from the Austrian Academy of Sciences via the impact project Charged Fusion Product Confinement in JET (BMWV grant GZ 4229/1-III/A/5/99). We are indebted to V. Drozdov (JET), D. Darrow (PPPL) and F. Paoletti (Columbia University) for providing the pertinent EFIT [2] equilibria for the considered discharges in JET and NSTX. Further we are grateful to F. Hofmann and J. Lister (CRPP-EPFL) for supplying the equilibrium data for the considered TCV discharges.

REFERENCES

- [1] V.D. Pustovitov, Plasma Phys. Rep., **24**, 279 (1998)
- [2] V.A. Yavorskij, K. Schoepf, et al., *Analytical Models of Axisymmetric Toroidal Magnetic Fields with Noncircular Flux Surfaces*, submitted to Plasma Phys. & Contr. Fusion

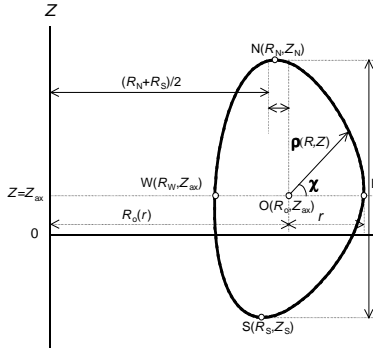


Fig.1: Coordinate system

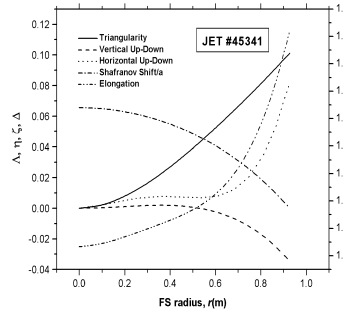


Fig.2: Profiles of flux surface parameters for JET shot # 45341 ($t \sim 45$ s)

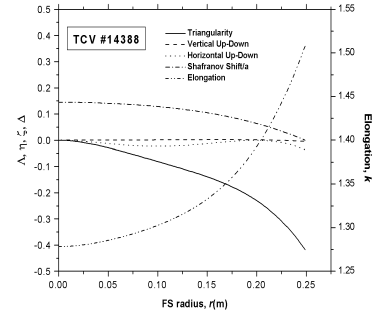


Fig.3: Profiles of flux surface parameters for TCV shot #14388

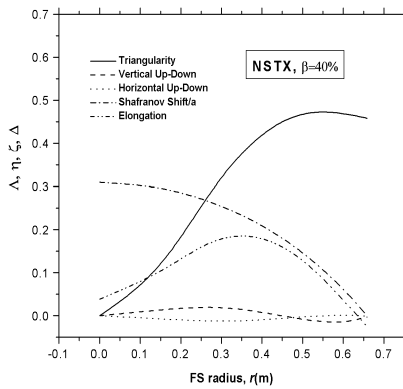


Fig.4: Profiles of flux surface parameters for NSTX at $\beta = 40\%$ (TRANSP run 11113P03 at $t = 1.15$ s)

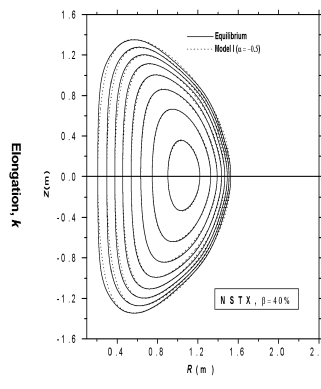


Fig.5: Comparison between real surfaces and model III for NSTX at $\beta = 40\%$

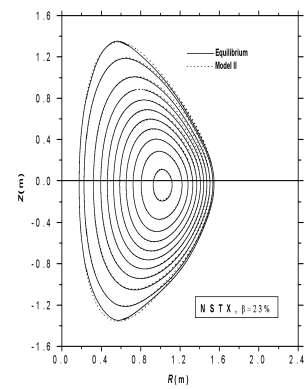


Fig.6: Comparison between real surfaces and model II for NSTX at $\beta = 23\%$

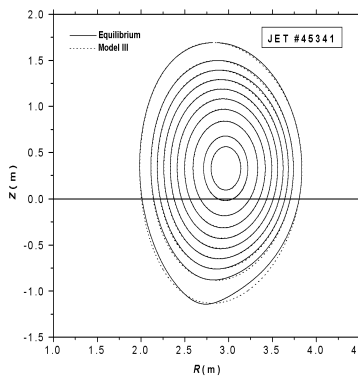


Fig.7: Comparison between real surfaces and best model (JET shot # 45341)

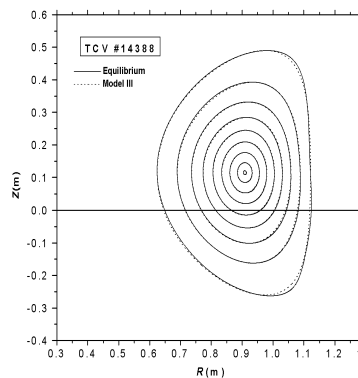


Fig.8: Comparison between real surfaces and best model (TCV shot #14388)

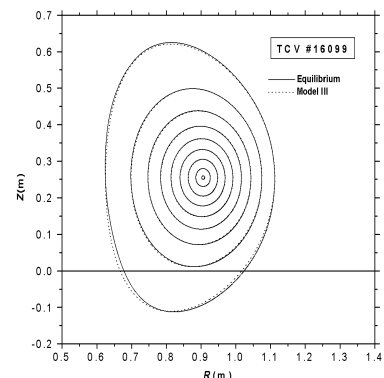


Fig.9: Comparison between real surfaces and best model (TCV shot #16099)